Rev. Roum. Sci. Techn.– Électrotechn. et Énerg.
Vol. **62**, *4*, pp. 388–393, Bucarest, 2017

ANALYSIS OF LEAKAGE INDUCTANCE FOR MULTI-ZONE INDUCTION HEATER

KALLOL BHAUMIK[1], AVIK DATTA[1], PRADIP KUMAR SADHU[2]

Key words: Multi-zone high frequency induction heating, Leakage inductance, Solenoid coil, PSIM.

This paper presents a multiple and multi-zone output induction heating system. It consists of a half bridge inverter followed by a bridge rectifier and a ring filter. The analysis of high-frequency leakage inductance at a particular frequency for air core solenoid has been performed neglecting all the mutual effect. Proposed circuit is designed in PSIM environment and simulated. A comparative study of the simulation results reveal that the RMS value of output current of the proposed circuit is changed when the working coils are magnetically coupled with the load impedances.

1. INTRODUCTION

Multi-zone and multi-coil or multiple output induction heating systems [1] are very effective to improve the heat distributions [2]. Multi-coil system is also applicable for simultaneous heating of different object [3]. Multiple output induction heating systems can be applied to both industrial and domestic application purpose [4]. Many researches are going on to find out efficient multi coil heating and some of these research methodology has been published containing calculation and efficient analysis [5–7].

Leakage inductive reactance [8] plays a critical role for the power electronic circuit. Switching losses and power efficiency are affected by the stored magnetic energy in the leakage inductance [9]. This leakage energy causes the voltage spikes and gives rise to the electromagnetic interference problems [10].

In high-frequency phenomenon leakage inductance is a frequency dependent parameter. Leakage inductance reduces [11] with increasing frequency [12]. That is why higher switching frequency is preferable to minimize the leakage energy. As the current increases gradually and causes non-uniform current distribution within the conductor changes.

The current density is high on the conductor surface at high frequency which leads to leakage magnetic field storage in cross sectional area of the conductors. Hence leakage magnetic field is reduced.

This paper focuses mainly on a comparative study among the results. Observation shows that the RMS value of the output current is lower when the working coils are magnetically coupled with the load impedances. On load condition of induction heating process shows the transformer phenomenon [12, 13].This paper consists of three major parts. First part contains the leakage inductance formula which is derived from diffusion equation, then a multi-coil induction heating system is proposed and the proposed circuit is simulated in PSIM environment.

2. CALCULATION OF LEAKAGE INDUCTANCE

The propagation of electromagnetic energy away from time varying sources in the form of waves can be predicted by Maxwell's equation.

In a source free region ($\rho = 0$, $J = 0$) Maxwell's equation can be written as,

$$\bar{\nabla} \times \bar{H} = \bar{J} + \frac{\partial \bar{D}}{\partial t} = \sigma \bar{E} + \varepsilon \frac{\partial \bar{E}}{\partial t}, \quad (1)$$

$$\bar{\nabla} \times \bar{E} = -\frac{\partial \bar{B}}{\partial t} = -\mu \frac{\partial \bar{H}}{\partial t}, \quad (2)$$

where:

$\bar{E}$ = electric field intensity,

$\bar{H}$ = magnetic field intensity,

$\bar{D}$ = electric flux density,

$\bar{B}$ =magnetic flux density,

σ = conductivity of the medium,

ε =permittivity of the medium,

μ = permeability of the medium,

$\bar{J}$ = current density,

$\frac{\partial}{\partial t}$ = first order partial differential operator with respect to time t,

$\bar{\nabla} = \hat{\mathrm{i}} \frac{\partial}{\partial x} + \hat{\mathrm{j}} \frac{\partial}{\partial y} + \hat{\mathrm{k}} \frac{\partial}{\partial z}$, where $\hat{\mathrm{i}}, \hat{\mathrm{j}}$ and $\hat{\mathrm{k}}$ are the unit vectors in the x, y and z direction in a rectangular Cartesian coordinate system.

Applying curl in both sides of the two equations, diffusion equation or Helmholtz's equations can be obtained.

$$\nabla^2 \bar{E} - \mu\varepsilon \frac{\partial^2 \bar{E}}{\partial t^2} - \mu\sigma \frac{\partial \bar{E}}{\partial t} = 0, \quad (3)$$

$$\nabla^2 \bar{H} - \mu\varepsilon \frac{\partial^2 \bar{H}}{\partial t^2} - \mu\sigma \frac{\partial \bar{H}}{\partial t} = 0. \quad (4)$$

The phasor form of the diffusion equation can be written as,

$$\nabla^2 \bar{E}_S = \mathrm{j}\,\omega\,\mu\,(\sigma + \mathrm{j}\,\omega\,\varepsilon)\,\bar{E}_S$$
$$\Rightarrow \nabla^2 \bar{E}_S - \gamma^2 \bar{E}_S = 0 \quad (5)$$
$$\nabla^2 \bar{H}_S = \mathrm{j}\,\omega\,\mu\,(\sigma + \mathrm{j}\,\omega\,\varepsilon)\,\bar{H}_S$$

[1] Indian School of Mines (under MHRD, Govt. of India), Research Scholar in Electrical Engineering Department, Dhanbad – 826004, India, E-mail: kallol_mid@yahoo.co.in
[2] Indian School of Mines (under MHRD, Govt. of India), Electrical Engineering Department, Dhanbad – 826004, India

$$\Rightarrow \nabla^2 \bar{H}_S - \gamma^2 \bar{H}_S = 0, \quad (6)$$

where: $\bar{E}_S$ = phasor electric field, $\bar{H}_S$ = phasor magnetic field, and

$$\nabla^2 = \frac{\partial^2}{\partial x^2} + \frac{\partial^2}{\partial y^2} + \frac{\partial^2}{\partial z^2},$$

$\gamma = \sqrt{j\omega\mu(\sigma + j\omega\varepsilon)}$ = propagation constant.

In order to solve the diffusion equations, Cartesian coordinates have been considered due to its symmetry. Let alignment of magnetic field ($\bar{H}_{ZS}$) is along the *z* axis. In other words magnetic field has only *Z* component. Here the magnetic field ($\bar{H}_{ZS}$) is the function of *x* axis only. Therefore the diffusion equations in phasor form become ordinary differential equation.

$$\frac{d^2 \bar{H}_{ZS}}{d x^2} = \gamma^2 \bar{H}_{ZS}. \quad (7)$$

For a magneto-quasi-static field,

$$\frac{d^2 \bar{H}_{ZS}}{dx^2} = \gamma^2 \bar{H}_{ZS} = j\omega\mu_0\sigma \bar{H}_{ZS}, \quad (8)$$

where: $\bar{H}_{ZS}$ = phasor magnetic field intensity along *z* axis, $\frac{d^2}{d x^2}$ = second order differential operator with respect to *x*.

Since the alignment of magnetic field ($\bar{H}_{ZS}$) is along the *z* axis and the propagation of the wave is along the *x* axis, the general solution of Helmholtz equation is given by

$$H(x) = H_1 e^{\gamma x} + H_2 e^{-\gamma x}, \quad (9)$$

where

H_1, H_2 = constant of the magnetic field, $\gamma = \sqrt{j\omega\mu_0\sigma} = \frac{1+j}{\delta}$, γ = propagation constant, where δ = skin depth

$$\delta = \frac{1}{\sqrt{\pi f \mu_0 \sigma}}$$

At 15 kHz skin depth (δ) and propagation constant (γ) of copper is given by $\delta = 0.411$, $\gamma = 3.43 \angle 45^0$.

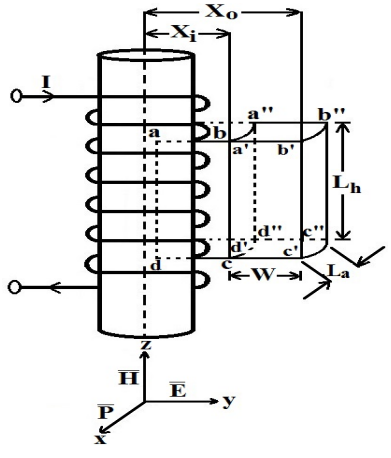

Fig. 1 – Leakage field of solenoid.

At steady condition the effective magnetic field exists inside the Amperian loop 'abcd' as shown in the above Fig. 1 and outside the Amperian loop the magnetic field is zero. In the above Fig. 1 $\bar{P}$ represents the direction of propagation of the wave along the *x* axis, $\bar{E}$ represents electric field intensity along the *y* axis and $\bar{H}$ represents magnetic field intensity along *z* axis. A three dimensional bounded space having the dimensions L_h, L_a and W has been considered which exists outside the Amperian loop 'abcd'. At high-frequency if any magnetic field exists outside the Amperian loop 'abcd' that means magnetic field exists inside the three dimensional bounded space, it is considered as leakage field. Hence the field constants are determined [14] by the boundary condition given below

$$H(x_i) = \frac{N I}{L_h}, \quad (10)$$

$$H(x_o) = 0, \quad (11)$$

where x_i and x_o are the distance from the centre to the outer surface of the coil and from the centre to the outside of the coil respectively.

The constants H_1 and H_2 of equation (9) can be determined by the given boundary condition.

$$H_1 = \frac{N I}{L_h} \frac{e^{-\gamma x_o}}{e^{-\gamma W} - e^{\gamma W}}, \quad (12)$$

$$H_2 = \frac{N I}{L_h} \frac{e^{\gamma x_o}}{e^{\gamma W} - e^{-\gamma W}}, \quad (13)$$

where $x_o - x_i = W$.

Applying the equations (12) and (13) into equation (9), the magnetic field exists inside the three dimensional bounded space in the Fig. 1 is obtained as follows

$$H(x) = \frac{NI}{L_h} \frac{\sinh(\gamma x)}{\sinh(\gamma W)}, \quad (14)$$

where x_0 is considered as *x*.

Therefore the stored energy inside the three dimensional bounded space is obtained as follows

$$H_i = \frac{1}{2} \mu_0 L_a L_h \int_0^W H(x)^2 dx = \frac{1}{2} \mu_0 L_a \frac{(NI)^2}{L_h} \frac{1}{\sinh^2(\gamma W)} \times \left[\frac{1}{4\gamma} \sinh(2\gamma W) + \frac{W}{2}\right]. \quad (15)$$

In general magnetic energy stored inside a volume is represented by

$$H_i = \frac{1}{2} L_{lk} I^2. \quad (16)$$

From equation (15) and (16) it can be written that,

$$L_{lk} = \frac{1}{2}\mu_0 L_a \frac{N^2}{L_h} \frac{1}{\sinh^2(\gamma W)} \times$$

$$\times\left[\frac{1}{4\gamma}\sinh(2\gamma W)+\frac{W}{2}\right], \qquad (17)$$

where L_{lk} = leakage inductance.

Table 1

Specification table for solenoid

Parameters	Values
No. of turns (N)	6
Height of the core (L_h)	26 mm
Mean turn length (L_a)	10 mm
Width (W)	10 mm
Propagation constant (γ)	3.43

Putting all the specification into equation (17), leakage inductance is determined as follows L_{lk} = 2.53 nH.

Therefore leakage reactance $X_{lk} = 2\pi f\ L_{lk}$ = 0.00024Ω. From the above results it is evident that the leakage inductance and hence leakage reactance of the air core solenoid at 15 kHz is very low. But in case of high-frequency transformer leakage reactance is higher [17]. That means under the influence of load amount of leakage field is higher since on load condition of the working coil is considered as transformer action.

3. PROPOSED CIRCUIT

An ac source is required to provide an alternating voltage to the working coil. Mainly three stages of operations are required for induction heating process. In this proposed circuit, supply power is first filtered by the ring filter (as shown in Fig. 3) and then rectified by the diode bridge rectifier.

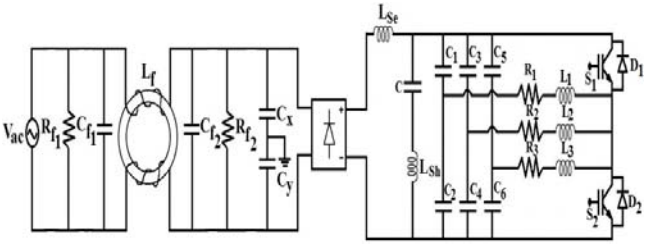

Fig. 2 – Multi-zone and multiple output induction heating system using half-bridge inverter.

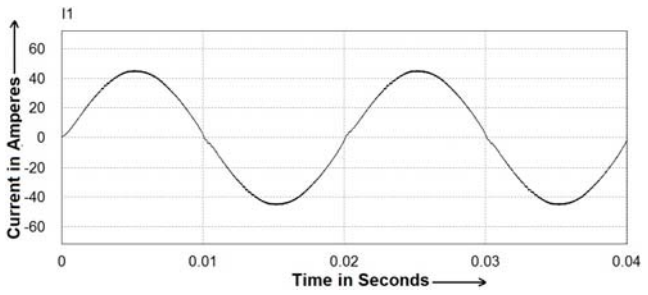

Fig. 3 – Sinusoidal input for diode bridge rectifier.

The steady state output from the diode bridge rectifier passes through a high frequency conversion stage. This is also known as the inversion stage. In this proposed circuit half-bridge inverter [15, 16] is used. Two insulated gate bipolar transistors (IGBTs) have been used as semiconductor switch. Two freewheeling diodes are connected parallel to the IGBTs to provide the discharging path of the energized coils. The output current of the inverter generates an alternating magnetic field into the working coil. As a consequence eddy currents are generated within the work piece and resistance leads to joule heating of the work piece. To generate a strong magnetic field, coil current must be very high (10–1 000 A).

Different modes of operation for the proposed circuit is shown below.

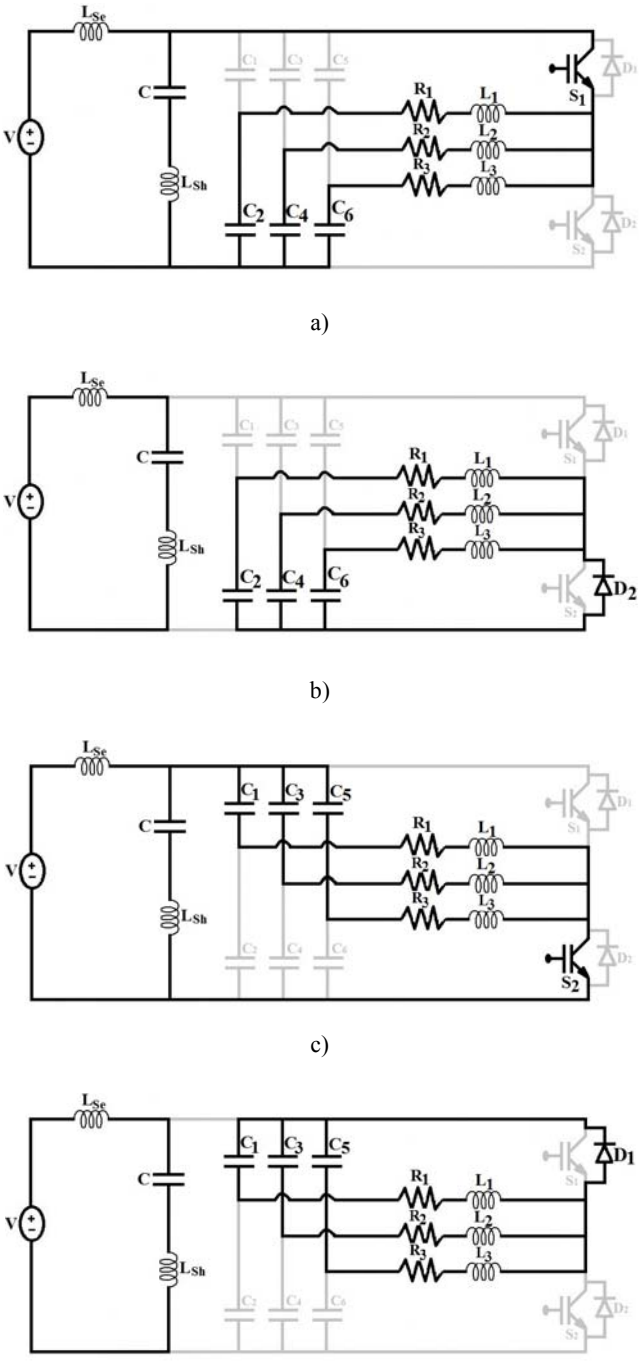

Fig. 4 – Operating modes for under: a) upper switch S_1 is on; b) upper switch S_1 is off; c) lower switch S_2 is on; d) lower switch S_2 is off.

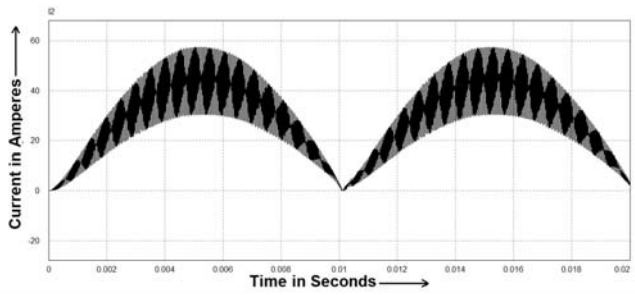

a)

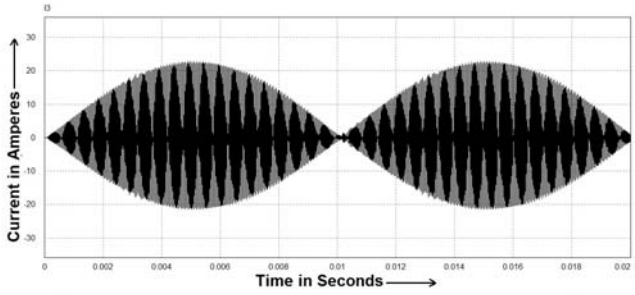

b)

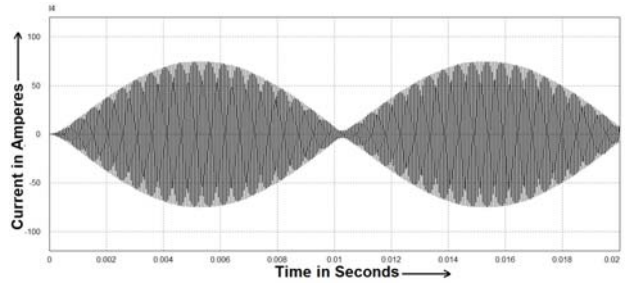

c)

Fig. 5 – Charging current waveform for: a) the coil L_{se}; b) the coil L_{sh}; c) coils L_1, L_2 and L_3.

Figure 5 demonstrates the corresponding waveforms for the different modes of operation as shown above.

On load condition all the coils of prior circuit can be replaced by a single phase transformer with series load as shown in Fig. 6a. Since on load condition transformer action takes place. The secondary terminal of the single phase transformer is connected to a series load which is the electrical equivalent model of induction heating load as depicted in Figs. 6b and 6c. The coil inside the proposed circuit depicted below (Fig. 7) signifies the secondary side referred to the primary side of the transformer.

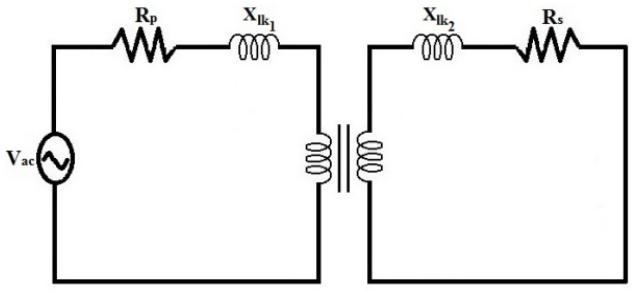

a)

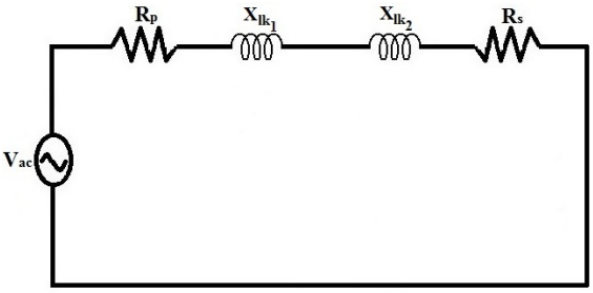

b)

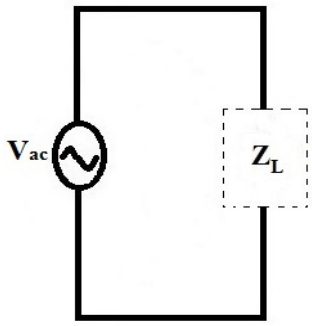

c)

Fig. 6 – Magnetic coupling of load: a) as a single phase transformer action; b) when secondary side is referred to primary; c) as equivalent load impedance.

From the above circuit total equivalent impedance (as shown in Fig. 5 can be calculated as

$$Z_L = \left(R_{\mathrm{e}} + \mathrm{j}X_{\mathrm{e}}\right),$$

where: a = turns ratio,

$$R_{\mathrm{e}} = R_{\mathrm{p}} + a^2 R_{\mathrm{s}},$$

$$X_{\mathrm{e}} = X_{lk_1} + a^2 X_{lk_2}.$$

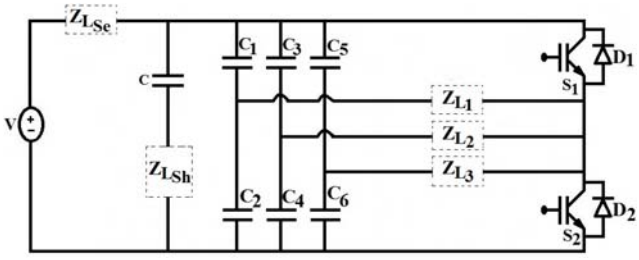

Fig. 7 – Multi-coil induction heating system with the coils replaced by a single phase transformer on load condition.

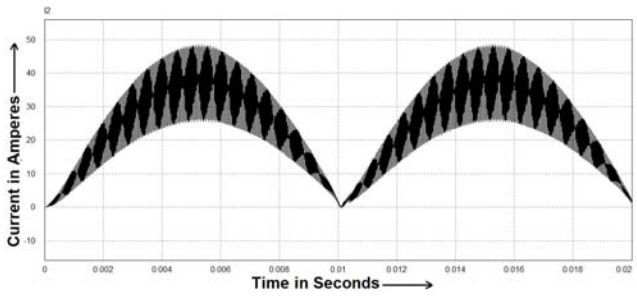

a)

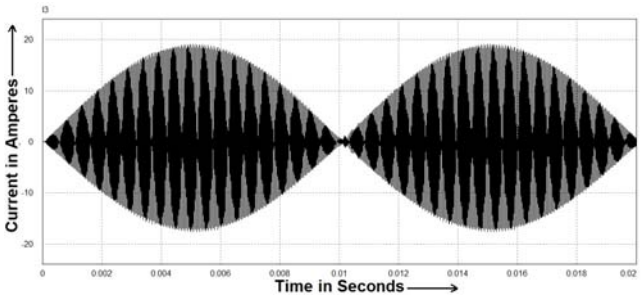

b)

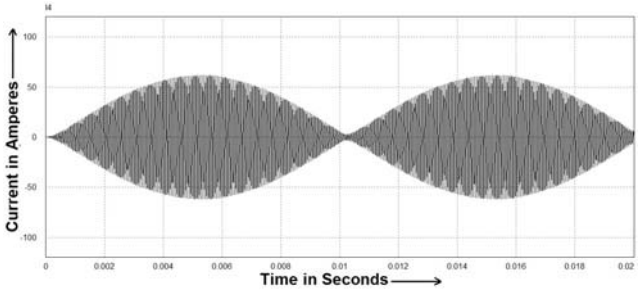

c)

Fig. 8 – Charging current waveform for: a) the coil Z_{Lse}; b) the coil Z_{Lsh}; c) coils Z_{L1}, Z_{L2} and Z_{L3}.

Figure 8 demonstrates the corresponding waveforms for the different modes of operation under the influence of load as shown above.

4. RESULTS AND DISCUSSIONS

The rms value of output current for the coils has been displayed in Table 2. It is evident that the rms value of the current is more when solenoid coil is used as working coil. As a matter of fact all the magnetic flux does not confined inside the magnetic core. Some of magnetic flux will come out from the core which is known as magnetic field leakage. The leakage inductance has been calculated in equation (17). From the newly derived expression it is evident that the leakage inductance for a solenoid inversely varied with the propagation constant. When working coil is under the influence of load acts as a transformer and the amount of leakage magnetic field is then more than the solenoid's leakage magnetic field. Therefore due to the presence of leakage field all the magnetic flux cannot be induced into another circuit. For this reason the rms value of load current is lower than the rms value of the main working coil.

The table which is displayed below represents the comparison between the currents at no load and on load condition.

Table 2

Comparison of simulation results

Type	Coil name	RMS value of current in Ampere
Solenoid	L_{se}	32.1
	L_{sh}	10.7
	L_1	37.6
	L_2	37.6
	L_3	37.6
Load Impedence	Z_{Lse}	27
	Z_{Lsh}	8.8
	Z_{L1}	30.9
	Z_{L2}	30.9
	Z_{L3}	30.9

5. CONCLUSION

This paper gives the idea of multi-zone and multiple output induction heating system which is suitable for uniform heat distribution and by using this system multiple heating objects can be heated simultaneously. At the same time expression of leakage inductance (equation 17) is derived and calculated for the solenoid coil which shows the low leakage field for the solenoid or helical coil. The derived expression is only applicable for the leakage field calculation of the solenoid coil at high-frequency. For the different geometrical shape of the coil, different leakage field equations can be derived by using the general diffusion equation under the specific boundary condition. Comparison of simulation results reveal that the effect of leakage field is reflected into the load current. But the reliability of the proposed circuit can be improved by using full bridge inverter topology.

ACKNOWLEDGEMENTS

Authors are thankful to the university grants commission, Bahadurshah Zafar Marg, New Delhi, India for granting financial support under Major Research Project entitled "Simulation of high frequency mirror inverter for energy efficient induction heated cooking oven using PSPICE" and also grateful to the Under Secretary and Joint Secretary of UGC, India for their active co-operation.

Received on December 17, 2016

REFERENCES

1. T. Leuca, Ş. Nagy, N.D. Trip, H. Silaghi, C. Mich-Vancea, *Optimal Design for Induction Heating using Genetic algorithms*, Rev. Roum. Sci. Techn. – Électrotechn. et Énerg., **60**, *2*, pp. 133–142 (2015).
2. P.H. Fujita, N. Uchida, K. Ozaki, *A new zone-control induction heating system using multiple inverter units applicable under mutual magnetic coupling conditions*, IEEE Trans. Power Electron., **26**, *7*, pp. 2009–2017 (2011).
3. F. Forest, E. Labouré, F. Costa, J.-Y. Gaspard, *Principle of a multi-load/single converter system for low power induction heating*, IEEE Trans. Ind. Electron., **15**, *2*, pp. 223–230, 2000.
4. O. Lucía, J.M. Burdío, L.A. Barragán, J. Acero, I. Millán, *Series resonant multi-inverter for multiple induction heaters*, IEEE Trans. Power Electron., **24**, *11*, pp. 2860–2868 (2010).
5. O. Lucía, I. Urriza, L.A. Barragan, D. Navarro, O. Jiménez, J.M. Burdío, *Real-time FPGA-based hardware-in-the-loop simulation test-bench applied to multiple output power converters*, IEEE Trans. Ind. Appl., **47**, *2*, pp. 853–860, 2011.
6. A. Chakraborty, P.K. Sadhu, K. Bhaumik, P. Pal, N. Pal, *Behaviour of a High Frequency Parallel Quasi Resonant Inverter Fitted Induction Heater with Different Switching Frequencies*, International Journal of Electrical and Computer Engineering, **6**, *2*, pp. 447–457 (2016).

7. O. Lucía, C. Carretero, D. Palacios, D. Valeau, J.M. Burdío, *Configurable snubber network for efficiency optimization of resonant converters applied to multi-load induction heating*, Electron. Lett., **47**, *17*, pp. 989–991 (2011).
8. W.G. Hurley , D.J. Wilcox, *Calculation of leakage inductance in transformer windings*, IEEE Trans. Power Electron., **9**, *1*, pp. 121–126 (1994).
9. J.-M. Choi, B.-J. Byen, Y.-J. Lee, D.-H. Han, H,-S, Kho, G.-H. Choe, *Design of leakage inductance in resonant DC-DC converter for electric vehicle charger*, IEEE Trans.Magn., **48**, *11*, pp. 4417–4420 (2012).
10. M. Lambert, F. Sirois, D.M. Martinez, J. Mahseredjian, *Analytical calculation of leakage inductance for low-frequency transformer modeling*, IEEE Trans. Power Del., **28**, *1*, pp. 507–515 (2013).
11. J. Zhang; Z. Ouyang; M. C. Duffy, M. A. E. Andersen, W. G. Hurley, *Leakage inductance calculation for planar transformers with a magnetic shunt*, IEEE Tran. Ind. Appl., **50**, *6*, pp. 4107–4112 (2014).
12. Chuang Bi, Hua Lu, Kelin Jia, Jingang Hu, Hui Li, *A Novel Multiple-Frequency Resonant Inverter for Induction Heating Applications*, IEEE Trans. Power Electron., **31**, *12*, pp. 8162–8171 (2016).
13. A. Stadler, M. Albach, *The influence of the winding layout on the core losses and the leakage inductance in high frequency transformers*, IEEE Trans. Magn., **42**, *4*, pp. 735–738 (2006).
14. X. Margueron, J.-P. Keradec, D. Magot, *Analytical calculation of static leakage inductances of HF transformers using PEEC formulas*, IEEE Trans. Ind. Appl., **43**, *4*, pp. 884–892 (2004).
15. M.K. Kazimierczuk, *High-Frequency Magnetic Components*, 2nd ed., Chichester, U.K., Wiley, 2009.
16. V.V.S.K. Bhajana, P. Drabek, M. Jara, *Performance Evaluation of LLC Resonant Full Bridge DC Converter for Auxiliary Systems in Traction*, Rev. Roum. Sci. Techn. – Électrotechn. et Énerg., **60**, *1*, pp. 79–88 (2015).
17. A. Bhattacharya, P.K. Sadhu, A. Bhattacharya, N. Pal, *Voltage Controlled Resonant Inverter – An Essential Tool For Induction Heated* Equipment, Rev. Roum. Sci. Techn. – Électrotechn. Et Énerg., **61**, *3*, pp. 273–277 (2016).
18. Ziwei Ouyang, Jun Zhang, William Gerard Hurley, *Calculation of Leakage Inductance for High-Frequency Transformers*, IEEE Trans. Power Electron., **30**, *10*, pp. 5769–5775 (2015).